BioNanoScience (2022) 12:1230–1237
https://doi.org/10.1007/s12668-022-01018-5

Fabrication of Amphotericin-B-loaded Sodium Alginate Nanoparticles for Biomedical Applications

Songul Ulag[1,2] · Sureyya Elif Celik[1,2] · Mustafa Sengor[1,2] · Oguzhan Gunduz[1,2]

Accepted: 26 July 2022 / Published online: 5 August 2022

Abstract
In this study, amphotericin-B (AMB)-loaded sodium alginate (SA) nanoparticles were fabricated using the electrospraying technique for biomedical applications. AMB is an antifungal agent and is poorly absorbed from the gastrointestinal tract due to its low aqueous solubility. Therefore, it should be given parenterally to treat systemic fungal infections. This study aims to transport it with nanoparticle formulations and observe the nanoparticle release behaviours. Scanning electron microscopy (SEM) images showed that nanoparticles of 0.5% SA fabricated at 37 kV had the most suitable particle diameter (93.36 ± 24.386 nm) for loading 0.5, 1, and 3 ml of AMB. Fourier transform infrared spectroscopy (FTIR) results demonstrated that AMB successfully loaded into 0.5% SA nanoparticles. Drug release behaviours of the AMB-loaded particles indicated that AMB was released with a burst at the beginning, and release behaviour became sustainable after half an hour. The encapsulation efficiencies of the different amounts of drug were calculated, and the results showed that the highest encapsulation efficiency belonged to the 0.5% SA/1 AMB nanoparticles (42 ± 1.23%).

Keywords Amphotericin-B · Biomedical · Drug release · Electrospraying · Nanoparticle · Sodium alginate

1 Introduction

Nanoparticles (NPs) are of great interest due to their unique physical and chemical properties and their use in biomedical materials. Since NPs contain materials designed at the atomic or molecular level, they are usually small-sized nanospheres [1]. Thus, larger materials can move more freely in the human body. Nanoscale particles exhibit unique structural, chemical, mechanical, magnetic, electrical, and biological properties. It can be said that nanostructures have gained much appreciation lately because they can be used as delivery agents by encapsulating drugs or adding therapeutic drugs and delivering them more precisely to target tissues in a controlled release [2, 3]. The unique physicochemical properties obtained by nano-sizing of materials attracted the attention of biomedical scientists, and the concept of nanopharmaceuticals emerged. Nanopharmaceuticals have been defined as pharmaceuticals designed at the nanoscale, i.e. pharmaceuticals in which the nanomaterial plays a key therapeutic role or adds additional functionality to the previous compound [4]. Nanocarrier-based drug delivery systems can overcome various challenges associated with oral administration routes, such as low-resolution drugs and control delivery within the desired time [5]. Polymeric nanoparticle-based drug delivery systems have the advantages such as scalability, targeted delivery, biocompatibility, biodegradability, and sustainable release of encapsulated drugs [6]. Polymeric NPs are particles with dimensions of 10–100 nm. Due to its small size, it is preferred in different areas due to its high volume-to-surface area ratio and adjustable dimensions [7]. Polymeric NPs can be produced by many techniques such as liposome capture, emulsification, coacervation, inclusion complexation, nanoprecipitation, emulsification-solvent evaporation, supercritical anti-solvent precipitation, spray drying, freeze-drying, and electrospraying. Among these techniques, the electrospray technique is one of the simplest and most versatile methods for producing nano and microparticles in recent years [8, 9]. Also, it is an easy and convenient method for forming polymeric particles with highly controlled sizes, distributions, non-traditional shapes, and unique surface morphologies that other methods

✉ Songul Ulag
ulagitu1773@gmail.com

[1] Center for Nanotechnology & Biomaterials Application and Research (NBUAM), Marmara University, Istanbul, Turkey

[2] Metallurgical and Materials Engineering, Faculty of Technology, Marmara University, Istanbul, Turkey

cannot achieve [10]. Therefore, this study aimed to fabricate NPs with the electrospray method to load the AMB and observe the AMB release behaviours from the SA nanoparticles. Alginate has been extensively studied due to its physical and chemical properties and use in forming (micro) particles and gels [11]. In addition, alginate is a preferred polymer for applications related to the controlled and targeted release of bioactive compounds [12, 13]. AMB is a polyene macrolide antifungal agent and is preferred for systemic fungal infection [14]. In this study, a nanotechnology-based approach to the development of AMB release and targeting systems was investigated. In this study, for the first time, AMB was loaded into the SA nanoparticles, and release behaviours were investigated.

2 Materials and Method

2.1 Materials

SA (molecular weight of 216.121 g/mol) and AMB (MW = 924.08 g/mol) were obtained from Sigma-Aldrich. Calcium chloride ($CaCl_2$, MW = 147.01 g/mol) was bought from Merck KGaA, Germany.

2.2 Fabrication of the 0.5% SA and 0.5% SA/AMB Solutions

Firstly, 0.5% SA powder was dissolved in 20 ml of distilled water and stirred at the magnetic stirrer at 300 rpm for an hour. Then, 0.5, 1, and 3 ml of AMB were added to this solution and waited for half an hour to provide the homogeneous distribution of the drug.

2.3 Physical Characterizations of the Electrosprayed Solutions

A standard 10-ml density bottle was used to measure the density values of the prepared solutions. The surface tension of the solutions was measured using a force tensiometer (Sigma 703D, Attension, Germany). The viscosity values of the solutions were calculated with a digital viscometer (DV-E, Brookfield, AMETEK, USA). The digital conductivity device (Cond 3110 SET-1, WTW, Germany) was used to determine the electrical conductivity values of the electrosprayed solutions [15, 16].

2.4 The Setup of the Electrospraying Process and Fabrication of Nanoparticles

A laboratory-scale electrospraying machine (NS24, Inovenso Co., Turkey) was used to fabricate the nanoparticles. A syringe pump (NE-300, New Era Pump Systems, Inc., USA) was used to adjust the flow rate of the solutions and connected to the stainless steel needle (inner diameter: 0.3 mm, outer diameter: 0.8 mm). Firstly, the polymer solution was placed into the 10-ml syringe, and then voltages ranging from 18 to 37 kV were applied between the needle and the collector. The distance between the needle tip and collector was adjusted by 12 cm after optimization. The flow rate value was optimized 0.03 ml/h value after optimization ranged from 0.01 to 0.05 ml/h flow rate values. During the electrospraying process, the lamellae filled with $CaCl_2$ solution (10 wt.% in distilled water) were used to collect the nanoparticles.

2.5 SEM Investigations of the Nanoparticles

The diameter and surface morphologies of the particles were observed by SEM (EVO MA-10, ZEISS). To prepare the samples for SEM, samples were vacuum coated with Au for 120 s, and images were taken at 10 kV. The Olympus analysis program was used to measure the diameters of the particles, which images were obtained from SEM [9].

2.6 FTIR Analysis

FTIR (4600 Jasco, Japan) was utilized to determine the nanoparticle chemical groups with a 4 cm^{-1} resolution, 32 cm^{-1} scan rate, and 4000–400 cm^{-1} wavenumber range. The powder nanoparticles were directly put onto the diamond tip of the FTIR, and before the analysis, the background of the air was taken. After each measurement, the diamond tip of the device was cleaned with 70% ethanol solution [9].

2.7 In Vitro *Drug Release Studies*

The release property of the AMB into the SA/AMB nanoparticles was carried out with phosphate-buffered saline

Table 1 Physical characterizations of the prepared solutions

Solutions	Density (g/cm^3)	Electrical conductivity (μS/cm)	Surface tension (mN/m)	Viscosity (mPa.s)
0.5% SA	1.001	1143.3 ± 6.65	48.84 ± 1.46	6562.3 ± 68.1
0.5% SA/0.5 AMB	1.0017	1016.3 ± 4.04	50.76 ±	4505.6 ± 421.9
0.5% SA/1 AMB	1.00	1160 ± 9.16	49.25 ± 0.62	8561.3 ± 430.8
0.5% SA/3 AMB	1.0039	1109.3 ± 1.52	47.46 ± 0.81	7648 ± 417.9

(PBS, pH 7.4) at 37 °C using a thermal shaker. The released AMB concentration was detected at different time intervals using a UV–Vis spectrophotometer (Shimadzu-Japan). The standard curve of the drug was determined at the scanning range of 190–600 nm using 2, 4, 6, 8, and 10 µg/ml drug amounts. Firstly, 5 mg powder nanoparticles were weighed

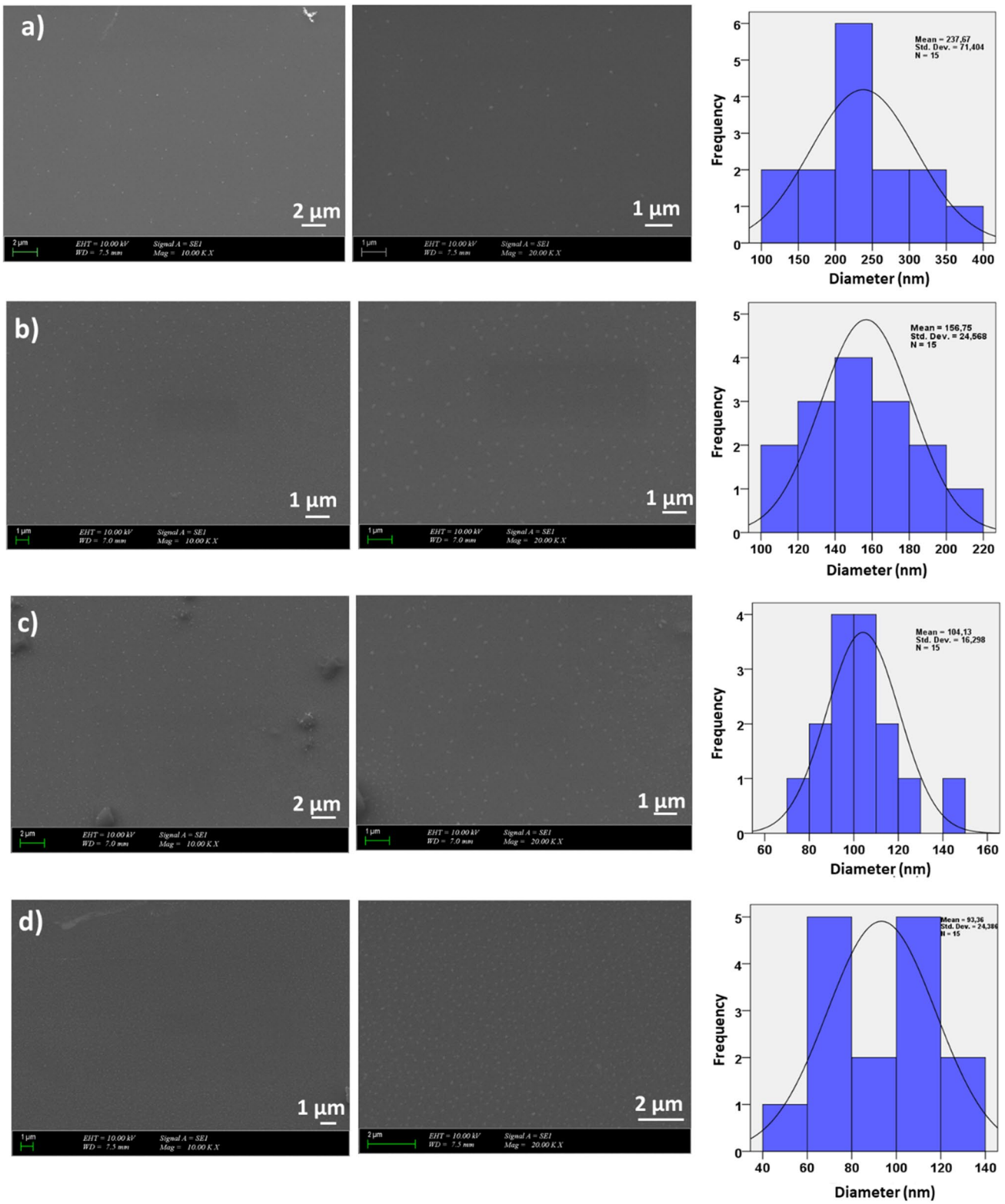

Fig. 1 The SEM images of the 0.5% SA with different voltage values: 23 kV (**a**), 28 kV (**b**), 30 kV (**c**), and 37 kV (**d**)

and put into the 2-ml eppendorf tubes, which have 1 ml PBS. These tubes were put into the thermal shaker, and measurements were taken for 15 min, 30 min, 1, 2, 3, 5, and 24 h. The fresh PBS was used after each measurement. The cumulative released behaviour was reported at 333.2 nm [17].

2.8 Encapsulation Efficiency of the AMB into Electrosprayed Nanoparticles

Encapsulation efficiency is defined as the ratio of actual drug loading to theoretical drug loading within nanoparticles. A standard assay procedure was used to determine the AMB content within the nanoparticles [16]. Briefly, the nanoparticles were utterly dissolved in the solvent, and UV detection at 333.2 nm was performed. In a measuring flask, AMB-loaded nanoparticles were weighted (5 mg) and dissolved in 10 ml of solvent (distilled water). The vial was gently mixed for 1 h to ensure complete dissolution of AMB from nanoparticles into the solvent. One milliliter of solution was taken and detected using a UV–visible spectrophotometer at 333.2 nm. The percentage of encapsulation efficiency was calculated using the equation given below. All measurements were repeated three times.

$$\text{Encapsulation efficiency} = \frac{mass\ of\ existent\ drug\ loaded\ in\ nanoparticles}{mass\ of\ used\ in\ fabricated\ nanoparticles}.100 \quad (1)$$

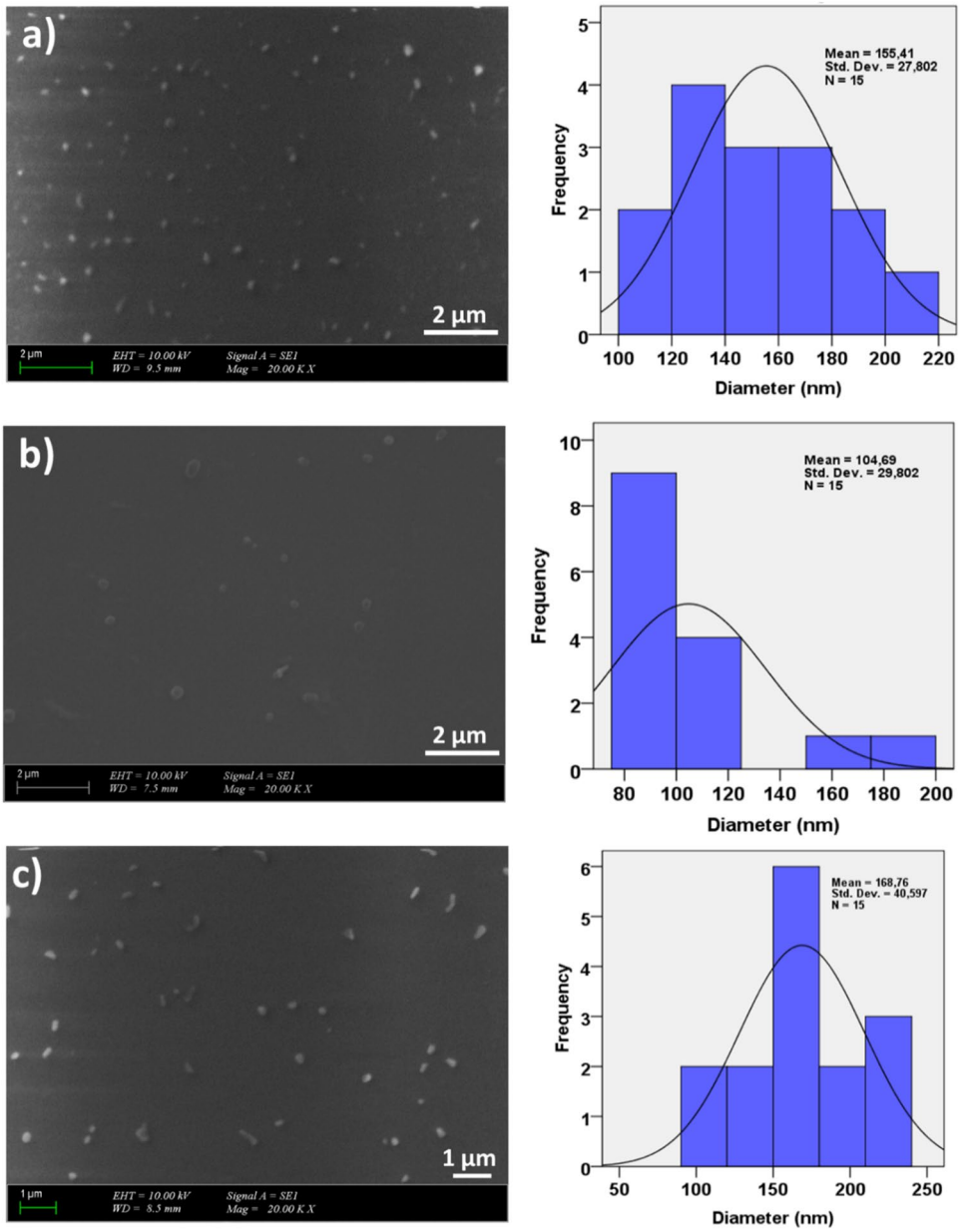

Fig. 2 The SEM images of the AMB-loaded 0.5% SA nanoparticles obtained at 37 kV: 0.5% SA/0.5 AMB (**a**), 0.5% SA/1 AMB (**b**), and 0.5% SA/3 AMB (**c**)

3 Results and Discussions

3.1 Solution Property Studies

The physical properties of the electrosprayed solutions, such as surface tension, electrical conductivity, viscosity, and density, which are some of the essential properties of the electrospray process, were measured and given in Table 1. It was observed that the density values of all solutions were nearly similar. The electrical conductivity decreased with 0.5 ml AMB addition but increased again with the addition of 1 ml AMB. Three milliliters of AMB addition also decreased the electrical conductivity value of the 0.5% SA. The lowest conductivity value belonged to the 0.5% SA/0.5 AMB. The viscosity values of sodium alginate can be separated into three parts which are low viscosity (< 240 mPa.s), medium viscosity (240–3500 mPa.s), and high viscosity (> 3500 mPa.s) [15]. The viscosity value found in this study was 6562.3 mPa.s. Thus, this value represented the high viscosity of 0.5% SA. By adding 0.5 ml AMB into the 0.5% SA, the viscosity value decreased and was found to be 4505.6 mPa.s. However, this value increased again with 1 and 3 ml of AMB. The 0.5% SA/1 AMB nanoparticles with the highest viscosity showed the lowest mean particle size. It is known that higher viscosity results in larger particle size. However, in these results, an increase in the particle size resulted in higher viscosity changes as compensated by the increased conductivity of the solution [18]. When the surface tension values of the solutions were examined, it was observed that the addition of AMB generally increased the surface tension, except for adding 3 ml AMB into the 0.5% SA. The surface tension value of 0.5% SA decreased from 48.84 to 47.46 mN/m with 3 ml AMB addition.

3.2 SEM Investigations

The surface morphologies of the 0.5% SA and AMB (0.5, 1, 3 ml) loaded 0.5% SA nanoparticles were examined using SEM. Figure 1 represents the particle shapes and diameters of the 0.5% SA nanoparticles fabricated at different voltage values in the optimization process. The all SEM images in Fig. 1 showed that particles had a uniform spherical shape and smooth surface. In Fig. 1a, b, 0.5% SA nanoparticles obtained at 18 kV showed a uniform structure, but a small number of particles were observed, and the primary particle diameter was 237.67 ± 71.404 nm. Figure 1c and d represented the SEM images of 0.5% SA nanoparticles obtained at 28 kV, and the results showed that they were monodisperse and their diameters were getting smaller (156.75 ± 24.568 nm). The nanoparticles fabricated at 30 kV were shown in Fig. 1e and f with their particle size distributions. The results reported that all particles had uniform shapes, and particles were dispersed homogeneously. The average particle size was found to be 104.13 ± 16.298 nm. The smallest particle size (93.36 ± 24.386 nm) was the 0.5% SA nanoparticles produced at 37 kV. Particles are both homogeneously dispersed and more numerous than other samples. According to the results, it can be reported that particle diameters decreased with increasing voltage values, and more homogeneous distributions were observed. Considering these results, the ideal voltage value for producing drug-loaded nanoparticles was determined as 37 kV. The SEM images of the AMB-loaded 0.5% SA nanoparticles are given in Fig. 2. Figure 2a represented the 0.5 ml AMB-loaded 0.5% SA nanoparticles and indicated that particles were numerous and had nearly uniform morphologies. The diameters of the particles were found as a mean value of 155.41 ± 27.802 nm. In Fig. 2b, the SEM images of the 1 ml AMB-loaded 0.5% SA nanoparticles were shown, and it was seen that particles were in small amounts and homogeneous distributions were not formed. Still, particle diameters (104.69 ± 29.802 nm) were smaller than 0.5 ml AMB-loaded nanoparticles. Figure 2c represented the 3 ml AMB-loaded 0.5% SA nanoparticles and reported that the particles were more numerous than the 1 ml AMB-loaded nanoparticles, but the particle diameter increased 168.76 ± 40.597 nm. Kaur et al. [19] fabricated AMB-loaded ethyl cellulose (EC) nanoparticles with the high-pressure emulsification-solvent evaporation (HPESE) method. They found that AMB-EC nanoparticles had 150 ± 9.23 nm mean particle size. This value was close to the results found in our study.

3.3 Chemical Properties of the Nanoparticles

FTIR analysis was carried out to investigate the chemical and molecular structures of the nanoparticles, and the

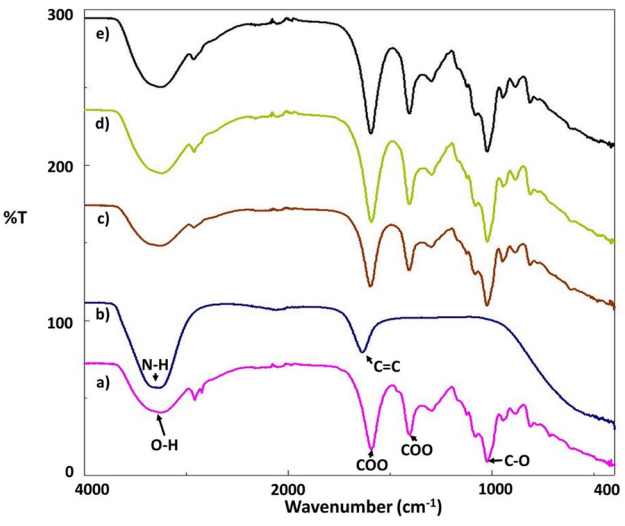

Fig. 3 The FTIR spectrums of the 0.5% SA (**a**), pristine AMB (**b**), 0.5% SA/0.5 AMB (**c**), 0.5% SA/1 AMB (**d**), 0.5% SA/3 AMB (**e**)

spectrum is shown in Fig. 3a. The 0.5% SA nanoparticle showed main peaks of pure SA, which were detected at 3259 cm^{-1} (vibration of the O–H group), 1590.99 cm^{-1} (stretching vibrations of the asymmetric COO group), 1405.85 cm^{-1} (symmetric –COO group), and 1024.02 cm^{-1} (C-O stretching vibrations) [20]. The FTIR spectrum of the pure AMB was shown in Fig. 3b, and the main peaks were observed at 3276.47 cm^{-1} and 1635.34 cm^{-1}, which belonged to the NH stretching of the primary aromatic amine and non-conjugated C = C stretching, respectively [21]. The peaks of 0.5% SA were more dominant for all the spectrums, and other than a few minor shifts in FTIR spectra, no significant change was observed with the addition of AMB into the 0.5% SA (Fig. 3 (c, d, e). This proved the homogeneous distribution of the different amounts of AMB in the 0.5% SA.

3.4 In Vitro *Release Examinations of the AMB from the Nanoparticles*

The release behaviour of AMB from the nanoparticles was examined in a PBS (pH: 7.4) for different time intervals. Figure 4A showed the calibration curve of the AMB using five solutions with proper concentrations (0.25, 0.5, 1, 1.5, and 2 µg/ml). By using the absorbance values at 333.2 nm in the calibration curve, the absorbance graph in Fig. 4B was obtained. Figure 4C demonstrated the cumulative release of the AMB from the nanoparticles. The graph showed that nearly 76.88, 66.14, and 59.06% of AMB were released from 0.5% SA/0.5 AMB, 0.5% SA/1 AMB, and 0.5% SA/3 AMB, respectively, at 15 min of immersion. After 30 min, the cumulative release of 0.5% SA/3 AMB nanoparticles reached 95.52%. After this time, the release behaviour continued almost the same for all nanoparticles. The

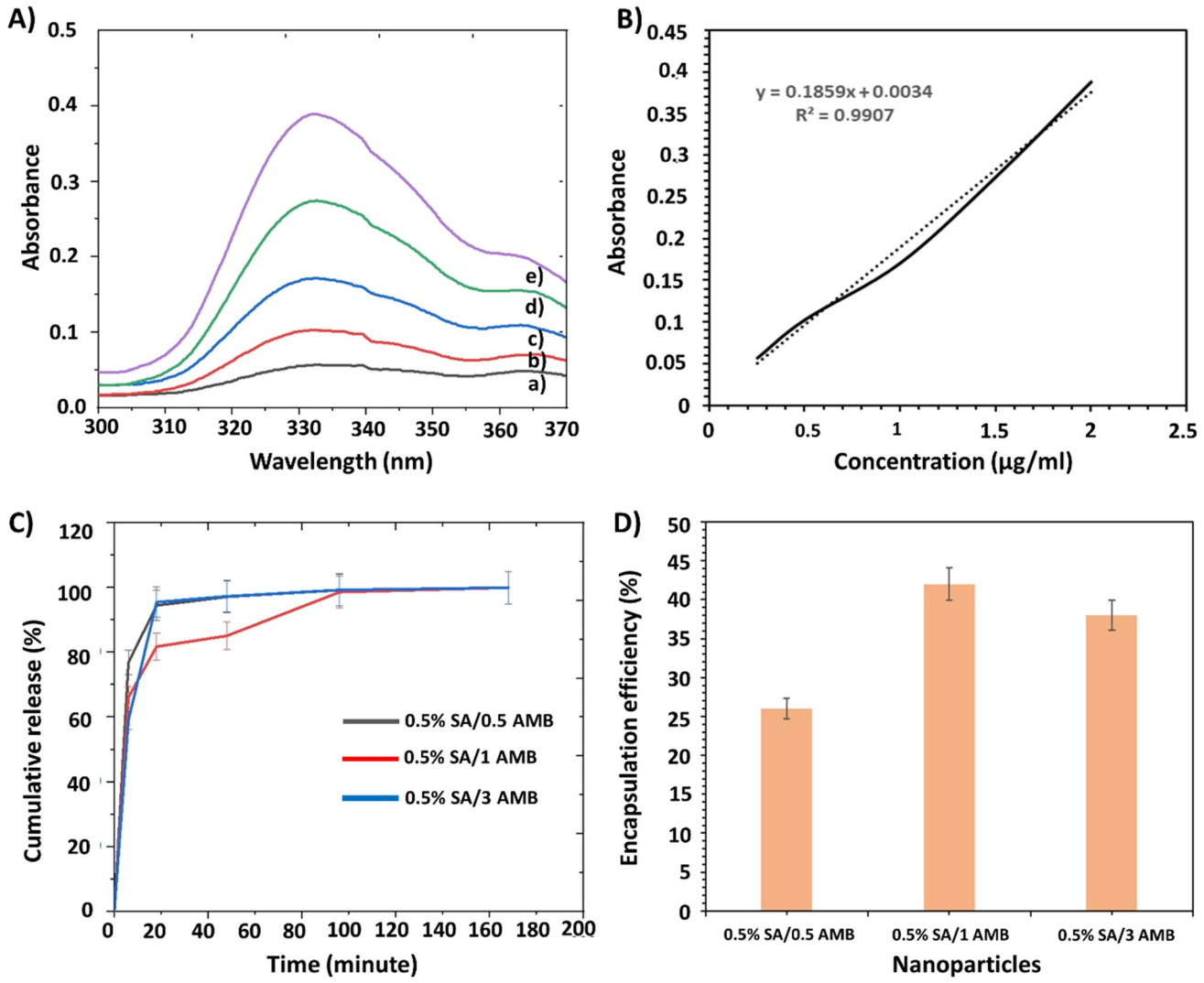

Fig. 4 The standard curve of the AMB (**A**): 0.25 µg/ml (**A**, a), 0.5 µg/ml (**A**, b), 1 µg/ml (**A**, c), 1.5 µg/ml (**A**, d), 2 µg/ml (**A**, e), the absorbance graph obtained at 333.2 nm (**B**), the cumulative release graph of the AMB (**C**), the percentages of encapsulation efficiency of AMB within the 0.5% SA nanoparticles (**D**)

initial burst release is beneficial for the release of antibiotic drugs, as it is necessary to destroy the spreading bacteria before they start to multiply. Therefore, for the few organisms that survive after the initial rapid release, a sustained release of antibiotics is required to prevent the remaining population [22]. The complete release occurred after 180 min of immersion for all the nanoparticles. Since the particle diameters of all nanoparticles were close to each other, the drug release behaviours were also similar.

The encapsulation efficiencies within the AMB-loaded nanoparticles were calculated, and the highest encapsulation efficiency for AMB-loaded nanoparticles was 0.5% SA/1 AMB with $42 \pm 1.23\%$. The lowest value was the 0.5% SA/0.5 AMB with $26 \pm 2.14\%$ encapsulation efficiency (Fig. 4D).

4 Conclusions

This study showed that uniform and monodisperse nanoparticles could be fabricated from SA polymer using the electrospray technique, and the AMB successfully loaded in SA nanoparticles. The diameters of the drug-loaded particles were ranged from 104 to 168 nm. FTIR spectrums proved the homogeneous distributions of the 0.5, 1, and 3 ml of AMB into the 0.5% SA solution. When the release results of the AMB used in different proportions were examined, it was observed that the release behaviour was almost the same for all concentrations. The 0.5% SA/1 AMB had the highest encapsulation efficiency compared to other particles. As a result, it can be said that these nanoscale drug-loaded particles are promising for biomedical applications.

Declarations

Ethical Approval This article does not contain any studies with human participants or animals.

Research Involving Humans and Animals Statement None.

Informed Consent None.

Conflict of Interest The authors have no competing interests.

References

1. Rudramurthy, G. R., Swamy, M. K., Sinniah, U. R., & Ghasemzadeh, A. (2016). Nanoparticles: Alternatives against drug-resistant pathogenic microbes. *Molecules, 21*, 836.
2. Jahangirian, H., Lemraski, E. G., Webster, T. J., Rafiee-Moghaddam, R., & Abdollahi, Y. (2017). A review of drug delivery systems based on nanotechnology and green chemistry: Green nanomedicine. *International Journal of Nanomedicine, 12*, 2957.
3. Mutlu, M. E., Ulag, S., Sengor, M., Daglılar, S., Narayan, R., & Gunduz, O. (2021). Electrosprayed collagen/gentamicin nanoparticles coated microneedle patches for skin treatment. *Materials Letters, 305*, 130844.
4. Bharathala, S., Sharma, P., (2019). Biomedical applications of nanoparticles. In: Kumar P and Singh S (ed) *Nanotechnology in Modern Animal Biotechnology Concepts and Applications*, Elsevier, 113–132.
5. Saqib, M., Bhatti, A. S. A., Ahmad, N. M., Ahmed, N., Shahnaz, G., Lebaz, N., & Elaissar, A. (2020). Amphotericin B loaded polymeric nanoparticles for treatment of Leishmania infections. *Nanomaterials, 10*, 1152.
6. Sridhar, R., & Ramakrishna, S. (2013). Electrosprayed nanoparticles for drug delivery and pharmaceutical applications. *Biomatter, 3*(3), e24281.
7. Adhikari, C. (2021). Polymer nanoparticles-preparations, applications and future insights: A concise review. *Polymer-Plastics Technology And Materials, 60*(18), 1996–2024.
8. Wang, P., Ding, M., Zhang, T., Wu, T., Qiao, R., Zhang, F., Wang, X., Zhong, J (2020). Electrospraying technique and its recent application advances for biological macromolecule encapsulation of food bioactive substances. *Food Reviews International*, 38 (4), 566–588.
9. Deniz, K. I., Ulag, S., & Gunduz, O. (2022). Investigation of the properties of encapsulated hydrophilic and hydrophobic drugs in whey protein microparticles. *Materials letters, 324*, 132664.
10. Saqib, M., Bhatti, A. S. A., Ahmad, N. M., Ahmed, N., Shahnaz, G., Lebaz, N., & Elaissari, A. (2020). Amphotericin B loaded polymeric nanoparticles for treatment of Leishmania infections. *Nanomaterials, 10*, 1152.
11 Paques, J. P., Linden, E., Rijn, C. J. M., & Sagis, L. M. C. (2014). Preparation methods of alginate nanoparticles. *Advances in Colloid and Interface Science, 209*, 163–171.
12. Pop, O. L., Leopold, L. F., Rugina, O. D., Diaconeasa, Z., Oprea, I., Tabaran, F., Tofana, M., Socaciu, C., Coman, C. (2016). Gold nanoparticles encapsulated in a polymeric matrix of sodium alginate. *Bulletin UASVM Food Science and Technology*, 73(2), 134.
13. Aranci, K., Uzun, M., Su, S., Cesur, S., Ulag, S., Amin, A., Guncu, M. M., Aksu, B., Kolayli, S., Ustundag, C. B., Silva, J. C., Ficai, D., Ficai, A., & Gunduz, O. (2020). 3D Propolis-sodium alginate scaffolds: Influence on structural parameters, release mechanisms, cell cytotoxicity and antibacterial activity. *Molecules, 25*(21), 5082.
14 Tiyaboonchai, W., & Limpeanchob, N. (2007). Formulation and characterization of amphotericin B–chitosan–dextran sulfate nanoparticles. *International Journal of Pharmaceutics, 329*, 142–149.
15. Devina, N., Eriwati, Y. K., & Santosa, A. S. (2018). The purity and viscosity of sodium alginate extracted from Sargassum brown seaweed species as a basic ingredient in dental alginate impression material. *Journal of Physics: Conference Series, 1073*, 052012.
16. Croitoru, A. M., Karacelebi, Y., Saatcioglu, E., Altan, E., Ulag, S., Aydoğan, H. K., Sahin, A., Motelica, L., Oprea, O., Tihauan, B. M., Popescu, R. C., Savu, D., Trusca, R., Ficai, D., Gunduz, O., & Ficai, A. (2021). Electrically triggered drug delivery from novel electrospun poly (lactic acid)/graphene oxide/quercetin fibrous scaffolds for wound dressing applications. *Pharmaceutics, 13*(7), 957.
17. Ulag, S., Ilhan, E., Demirhan, R., Sahin, A., Yilmaz, B. K., Aksu, B., Sengor, M., Ficai, D., Titu, A. M., Ficai, A., & Gunduz, O. (2021). Propolis-based nanofiber patches to repair corneal microbial keratitis. *Molecules, 26*(9), 2577.
18. Göttel, B., Lucas, H., Syrowatka, F., Knolle, W., Kuntsche, J., Heinzelmann, J., Viestenz, A., Mäder, K. (2020). In situ gelling amphotericin B nanofibers: A new option for the treatment of keratomycosis. *Frontiers in Bioengineering and Biotechnology*, 21, 1–16.
19. Kaur, K., Kumar, P., & Kush, P. (2020). Amphotericin B loaded ethyl cellulose nanoparticles with magnified oral bioavailability

for safe and effective treatment of fungal infection. *Biomedicine & Pharmacotherapy, 128*, 110297.
20. Ilhan, E., Ulag, S., Sahin, A., Yilmaz, B. K., Ekren, N., Kilic, O., Sengor, M., Kalaskar, D. M., Oktar, F. N., & Gunduz, O. (2021). Fabrication of tissue-engineered tympanic membrane patches using 3D-Printing technology. *Journal of the Mechanical Behavior of Biomedical Materials, 114*, 104219.
21. Ghosh, S., Das, S., De, A. K., Kar, N., & Bera, T. (2017). Amphotericin B-loaded mannose modified poly (D, Llactide-co-glycolide) polymeric nanoparticles for the treatment of visceral leishmaniasis: In vitro and in vivo approaches. *RSC Advances, 7*, 29575.
22. Altun, E., Yuca, E., Ekren, N., Kalaskar, D. M., Ficai, D., Dolete, G., Ficai, A., & Gunduz, O. (2021). Kinetic release studies of antibiotic patches for local transdermal delivery. *Pharmaceutics, 13*(5), 613.